Robust point-process Granger causality analysis in presence of exogenous temporal modulations and trial-by-trial variability in spike trains.

Short title: Functional connectivity with unobserved sources of variability in spiking neurons.

Antonino Casile[1,2*], Rose T. Faghih[3], Emery N. Brown[4]

1 Istituto Italiano di Tecnologia, Center for Translational Neurophysiology, Ferrara, FE, Italy
2 Harvard Medical School, Department of Neurobiology, Boston, MA, USA
3 Department of Electrical and Computer Engineering, University of Houston, Houston, TX, USA
4 Department of Brain and Cognitive Science, Massachusetts Institute of Technology, Cambridge, MA, USA

* antonino.casile@iit.it, toninocasile@gmail.com

Abstract

Assessing directional influences between neurons is instrumental to understand how brain circuits process information. To this end, Granger causality, a technique originally developed for time-continuous signals, has been extended to discrete spike trains. A fundamental assumption of this technique is that the temporal evolution of neuronal responses must be due only to endogenous interactions between recorded units, including self-interactions. This assumption is however rarely met in neurophysiological studies, where the response of each neuron is modulated by other exogenous causes such as, for example, other unobserved units or slow adaptation processes.

Here, we propose a novel point-process Granger causality technique that is robust with respect to the two most common exogenous modulations observed in real neuronal responses: within-trial temporal variations in spiking rate and between-trial variability in their magnitudes. This novel method works by explicitly including both types of modulations into the generalized linear model of the neuronal conditional intensity function (CIF). We then assess the causal influence of neuron i onto neuron j by measuring the relative reduction of neuron j's point process likelihood obtained considering or removing neuron i. CIF's hyper-parameters are set on a per-neuron basis by minimizing Akaike's information criterion.

In simulated data, the proposed method recovered with high accuracy the underlying ground-truth connectivity pattern. Application of presently available point-process Granger causality techniques produced instead a significant number of false positive connections. In real spiking responses recorded from neurons in the monkey pre-motor cortex (area F5), our method revealed many causal relationships between neurons as well as the temporal structure of their interactions. Given its robustness our method can be effectively applied to real neuronal data. Furthermore, its explicit estimate of the effects of unobserved causes on the recorded neuronal firing patterns can help decomposing their temporal variations into endogenous and exogenous components.

Author summary

Modern techniques in Neuroscience allow to investigate the brain at the network level by studying the flow of information between neurons. To this end, Granger causality has been extended to point process spike trains. A fundamental assumption of this technique is that there should be no unobserved causes of temporal variability in the recorded spike trains. This, however, greatly limits its applicability to real neuronal recordings as very often not all the sources of variability in neuronal responses can be concurrently recorded.

We present here a robust point-process Granger causality technique that overcome this problem by explicitly incorporating unobserved sources of variability into the model of neuronal spiking responses. In synthetic data sets, our new technique correctly recovered the underlying ground-truth functional connectivity between simulated units with a great degree of accuracy. Furthermore, its application to real neuronal recordings revealed many causal relationships between neurons as well as the temporal structure of their interactions.

Our results suggest that our novel Granger causality method is robust and it can be used to study the flow of information in the spiking patterns of simultaneously recorded neurons even in presence of unobserved causes of temporal variability.

Introduction

Modern neurophysiological recording techniques allow to simultaneously probe the activities of tens to hundreds neurons [1–3]. The availability of these high-dimensional data sets allows to address novel and relevant research questions about the brain. A particularly important question is to investigate brain functions at the circuit level, by assessing the flow of information between neurons. To this end, several analytical tools have been proposed in the past, such as cross-correlogram [4], joint peri-stimulus histogram [5] or gravitational cluster [6]. While providing noteworthy insights, these tools have also limitations as (1) they do provide little information about the directionality of discovered interactions and (2) they do not usually consider the point-process nature of neuronal spike trains. To overcome both issues Kim et al. proposed an extension of Granger causality to point processes [7].

Granger causality is an analytical tool originally proposed in the context of econometric time series [8]. A stochastic process x is said to Granger causally influence another process y (henceforth denoted with $x \to y$) if knowledge of values of x at times before t improves, in a statistically significant manner, the prediction of y at time t beyond inclusion of past values of y itself. Granger causality assumes that all sources of temporal modulations of the processes x and y must be endogenous to the set of considered processes. That is, they must be entirely explained by the processes' past histories and there should be no common unobserved driver of temporal variability [9]. However, this is often not the case in neurophysiological experiments where many of the causes that produce temporal modulations in neuronal responses are exogenous to the ensemble of recorded neurons. Indeed, the activity of a neuron at each time point results from the integration of signals coming from many, potentially thousands, other neurons, most of which are not concurrently recorded. Furthermore, in many experimental settings, we are interested in the so-called *functional connectivity* between neurons. That is, the amount and directionality of information flow when the brain state, is perturbed by an event (e.g. sensory stimulation or motor behavior). Under these conditions, neurons exhibit temporal modulations in the statistics of their firing patterns that are due to the interactions with neighboring neurons located in the their local network as well as more distant units in projecting brain regions. Finally, the

magnitude of neuronal responses often exhibits a physiological, potentially correlated, trial-by-trial variability, that brings the system further away from the conditions assumed by Granger causality.

In this paper, we show that, in the presence of exogenously temporally modulated and trial-by-trial variable spike trains the point-process Granger causality technique proposed by Kim et al. [7] might recover inaccurate patterns of connectivity. We then propose two novel methods that address this issue. The first method, called G-ETM, is designed to extend point-process Granger causality to spike trains whose magnitudes are modulated by exogenous causes. The second method, called G-ETMV, is computationally more demanding but it recovers the correct pattens of functional connectivity between a set of interconnected neurons exhibiting both trial-by-trial variability and exogenous temporal modulations in their firing patterns. We show the effectiveness of our new Granger causality techniques by means of quantitative computer simulations and application to real spike trains recorded from the monkey pre-motor cortex (area F5).

Results

Throughout this section we will denote as *endogenous*, temporal modulations in neuronal responses that are due to interactions between the recorded neurons (including self-interactions) and as *exogenous*, temporal modulations that are due to unobserved causes.

Standard point-process Granger causality fails with spike trains exhibiting exogenous temporal modulations

To show how standard point-process Granger causality can produce incorrect patterns of connectivity in the presence of spike trains exhibiting exogenous temporal modulations, we applied Kim et al.'s Granger method to 40 simulated trials (Fig. 1 A) of a simple system consisting of two units. The two units were not functionally connected as their spike trains were generated by means of two independent Poisson processes (Fig. 1 B). Furthermore, within each trial, they underwent an exogenous bell-shaped modulation of their firing rates. Responses like these might be recorded, for example, in motor areas during the execution or preparation of actions (see for Example Fig. 2 in [10]). In these cases one obvious question that arises is whether the two units represent subsequent stages of cortical processing, and their responses are thus causally related, or if they are independently driven by an external, unobserved source.

This relevant question represents a natural application of the Granger causality framework. Application of Kim et al.'s method to the spikes trains in Fig. 1 A revealed many causal connections that, although statistically significant, were not actually present in our system (compare the ground-truth connectivity in Fig. 1 B with the recovered connectivity in Fig. 1 C). To see why this happened we have to consider the estimates of the interaction functions (the γ terms in Eq. 2, Fig. 1 D). In the Granger framework, interaction functions describe how the past history of all neurons at different time lags modulate, at each time point, the activity of a given neuron. In our example, their ground-truth values are identically zero for all neurons and time lags as there is no mutual or self interaction at any time lag between the two simulated units. However, not only their estimated values are different from zero at several time lags, but, in many cases, these differences are also statistically significant (red dots in Fig. 1 D). This happened because, the GLM fitting process assigned the variance produced by the temporal modulations of the spike trains to the only available free parameters. That is, those related to interactions between neurons (the γ terms in Eq. 2). For the specific

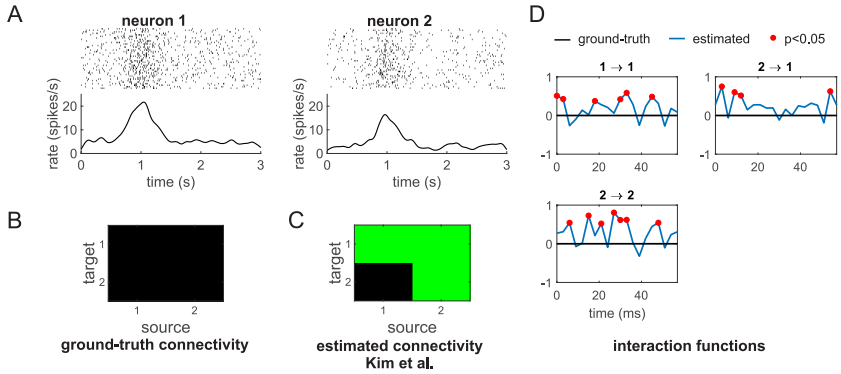

Figure 1. Standard Granger causality fails with spike trains exhibiting exogenous temporal modulations. (A) Spike trains of two units simulated by means of two independent Poisson processes. In the top panels, each row represent a trial (a total of 40 trials were generated) and each vertical line a spike. The bottom panels show the average firing rate across trials. On each trial, each neuron underwent a bell-shaped modulation of its firing rate centered around $t = 1\ s$ and with a temporal width of 200 ms. (B) Ground-truth connectivity of the two units. In this representation a green square represents a significant causal connection from the source to the target unit, while a black square signifies no causal connection between them. Since the two units are independent the ground-truth connectivity matrix contains, in this case, only black squares. (C) Connectivity recovered by the point process Granger causality technique proposed by Kim et al. [7]. The recovered connectivity matrix contains three fictitious connections: $1 \rightarrow 1$, $1 \rightarrow 2$ and $2 \rightarrow 1$. (D) Ground-truth values (black curves) and estimates (blue curves) of the interaction functions for the significant functional connections. Red dots mark values that are significantly different from 0 at $p < 0.05$.

data set of Fig. 1 A, inclusion of fictitious causal influences $1 \rightarrow 1$, $2 \rightarrow 2$ and $2 \rightarrow 1$ could indeed explain a significant fraction of this variance. This result is not only incorrect but also not robust. Different data sets, generated according to the same CIFs as those in Fig. 1, will, in general, produce different fictitious patterns of causal connectivity.

Extending point-process Granger causality to spike trains exhibiting exogenous temporal modulations

To overcome this problem we propose here G-ETM (Granger causality with Exogenous Temporal Modulations): a novel model that extends the computation of Granger causality to spike trains exhibiting exogenous temporal modulations. To this end, we exploited the organization of neurophysiological experiments into trials and the consistency, across trials, of temporal changes in firing rates to divide, for each neuron i, the duration T of each trial into N_i non-overlapping windows. Within each window, we model the CIF of a given neuron i as the sum of a *baseline* rate of activity and the sum of the influences of all other neurons in the ensemble (including neuron i itself). Having one additional parameter for each interval allows us to explicitly take into account transient changes in the CIF of neurons due to exogenous, unobserved factors.

Application of G-ETM to the spike trains of Fig. 1 produced the correct pattern of causal connectivity (Fig. 2 A). Furthermore, our technique produced also an estimate of the exogenous temporal modulations of the two simulated units that correctly captured their ground-truth values (Fig. 2 B). This happened because we now explicitly model

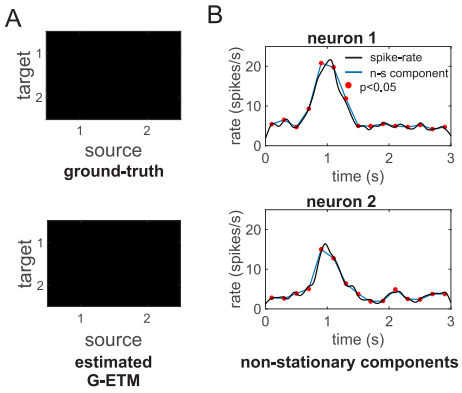

Figure 2. Application of our G-ETM Granger causality method to the spike trains of Fig. 1. (A) ground-truth (upper panel) and recovered (bottom panel) connectivity matrices. (B) Estimated (blue curves) and ground truth (black curves) interaction functions. (C) Estimates of the exogenous components of firing patterns. That is, changes in firing rates that are not due to interactions with other neurons. Symbols are as in Fig. 1.

exogenous temporal changes of firing rates by means of the terms $\gamma_{k,q}$ in Eq. 4. Therefore, the GLM fitting process no longer needs to generate fictitious connections to explain the variance that they produce.

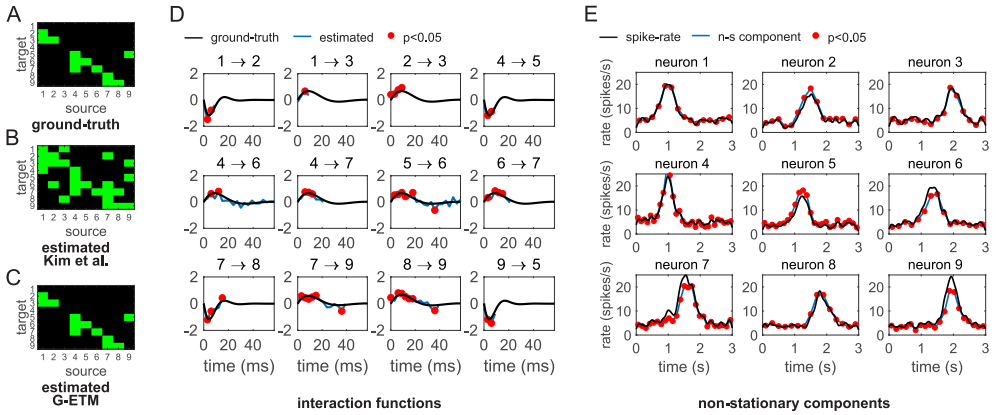

Figure 3. Application of G-ETM to a complex system. (A) Ground-truth connectivity pattern. (B) Connectivity pattern estimated by applying Kim et al.'s method [7]. (C) Connectivity pattern estimated by means of our G-ETM method. (D) Estimated (blue curves) and ground-truth (black curves) interaction functions of the significant causal connections. (E) Estimates of the exogenous components of firing patterns. Symbols are as in Figs. 1 and 2.

We next evaluated G-ETMon a more complex system composed of 9 units subdivided into two disjoint (i.e. not interacting) subsets: units 1-3 and 4-9 (Fig. 3 A) respectively. Within each simulated 3 s trial, units' firing patterns were determined by (1) influences from other units in the same subset and (2) bell-like exogenous stimulation that for each unit peaked at a different time in the interval between $t = 1\ s$ and $t = 2\ s$. This example is meant to model the case of simultaneous recordings from two areas during occurrence of an experimental event. In this setting, the question arises of whether there is any functional connectivity between the two recorded areas and, if so, what is its directionality. In our simulated network, there was no direct

connectivity between the two *areas* (i.e. the two subset of units). Application of Kim et al.'s method provided an inaccurate estimate of the local pattern of the connectivity both within and between the two subsets of units (Fig. 3 B). In particular, it produced several additional false-positive connections suggesting an incorrect pattern of *inter-area* connectivity. In an experimental setting, this pattern of result would provide support for the incorrect conclusion of a functional connectivity between the two *areas*. On the contrary, G-ETM recovered the correct pattern of causal connectivity both within and between the two subsets of units (Fig. 3 C). Furthermore, it also provided an accurate estimate of the interaction functions between units (Fig. 3 D). It is worth noting that temporal changes in the units' firing rates were almost entirely due to exogenous stimulation (Fig. 3 E). This means, that our method was sensitive enough to detect influences between units, even when, as is often the case for real neurons, they produced only minimal changes in their firing rates.

To provide a more general and thorough validation of G-ETM we performed a series of Montecarlo simulations (Fig. 4). To this end, we simulated 40 trials of a network consisting of 4 neurons and 6 connections whose placement (i.e. connected nodes and directionality of the connection), type (i.e. excitatory or inhibitory) and strength were randomly determined (but did not change across trials). In addition to mutual and self influences the spike rates of the 4 neurons underwent also an exogenous bell-shaped modulation. For each neuron the modulation peaked always at the same time that was however different across neurons and distributed in the interval $t = 1\ s$ and $t = 2\ s$. We then estimated causal connectivity by applying both Kim et al.'s and our method and compared these two connectivity patterns with the known ground-truth connectivity (Fig. 4 A). We iterated this procedure 100 times randomly determining the network structure at each run. Consistent with the intuition provided by Figs. 1 and 3 application of Kim et al's method produced false positives (i.e. deeming a connection significant when it is not present in the network) in 42 % of the cases, which exceeds by almost 10-fold the set statistical threshold of $p < 0.05$ (Fig. 4 B). On the contrary, G-ETM not only provided a comparably good estimate of the connectivity pattern (85 % vs. 88 % correct for our and Kim et al.'s methods respectively) but also produced a percentage of false positives compatible with the selected statistical threshold (4.2 %, Fig. 4 B). These results further show that G-ETM provides an accurate estimate of the causal influences in a network of neurons in the presence of exogenous temporal modulations of their firing rates.

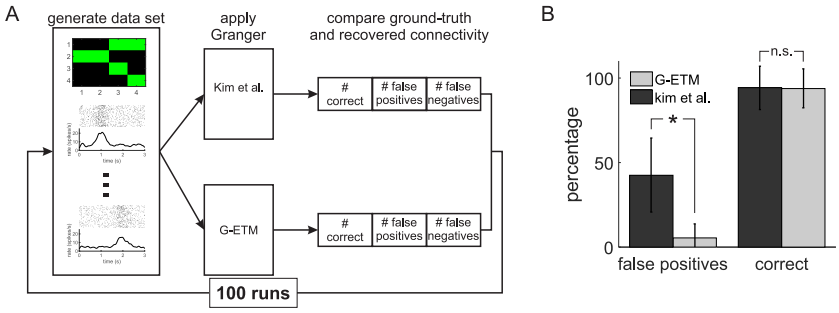

Figure 4. Montecarlo validation of G-ETM (A) Pictorial exemplification of our procedure (see main text for further details). In brief, we first randomly generated a connectivity pattern in a network of 4 neurons. We then applied Kim et al.'s and G-ETM Granger techniques to a data set consisting of 40 simulated trials for each neuron. Finally, we compared ground-truth connectivity with that estimated by the two methods. (B) We repeated this procedure for 100 runs to estimate the percentage of correct and false positive connections recovered by the two methods. Statistically significant differences are marked by an asterisk.

Application to real spike train data

In a further step we applied G-ETM to real spike-train data. To this end, we simultaneously recorded the response of 12 neurons from the monkey pre-motor cortex (area F5) during the preparation of goal-directed motor acts. The task of the monkey was to attend to a briefly flashed cue indicating a to-be-executed action and to withhold movement execution until a subsequent go signal occurring on randomly between 0.8 and 1.2s after cue onset. Fig. S1 shows the responses of the 12 recorded neurons during this motor preparation period. In each panel, $t = 0$ marks cue presentation.

We collected data from a total of 57 trials and analyzed neuronal responses recorded in the interval from 0.5 s before until 1 s after cue presentation. Consistent with previous studies of monkey pre-motor cortex [11], the responses of neurons in area F5 were significantly modulated by the preparation of a motor act, exhibiting both phasic and transient modulations in their firing rates (Fig. S1). We applied G-ETM to these spike trains. The results of our analysis revealed a complex pattern of Granger connectivity with both self- and mutual interactions between the recorded neurons (Fig. 5A). Application of Kim et al.'s method recovered a different pattern of connectivity exhibiting a higher number of mutual influences between neurons (off-diagonal elements in Fig. 5B). Although in this case, we do no have the ground-truth connectivity pattern, quantitative simulations reported in Figs. 3 and 4 strongly suggest that these additional causal connections are likely false positives.

Interestingly, examination of the recovered interaction functions (Fig. 5C) suggests that both self- and mutual interactions are time-dependent with a general trend of being inhibitory at shorter time scales and excitatory at longer time scales. Finally, examination of the recovered exogenous components of the firing patterns (Fig. 5D) shows that for some units (e.g. units 6 or 11) their temporal modulations could be only partially explained by exogenous influences and the remaining part was explained by self- or mutual interactions with other units. This result suggests that, in addition to recovering patterns of causal connectivity, G-ETM can be also effectively used to decompose the firing pattern of recorded units into exogenous (i.e. due to unobserved units) and endogenous (i.e. due to observed units) components.

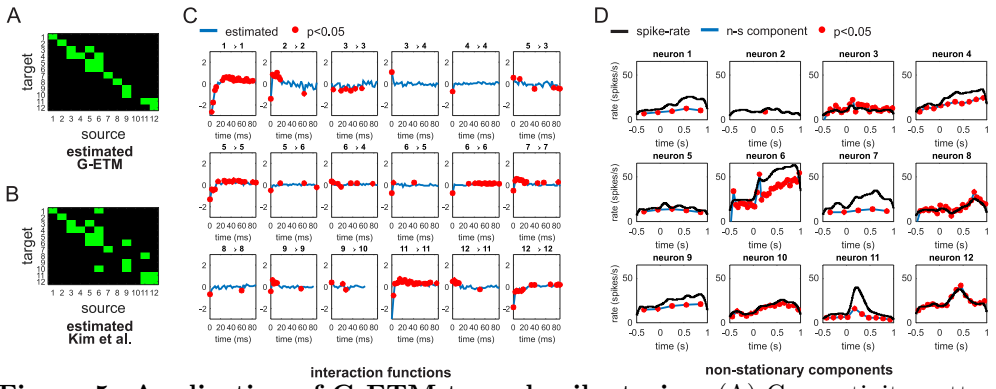

Figure 5. Application of G-ETM to real spike trains. (A) Connectivity pattern estimated by our G-ETM method. (B) Connectivity pattern estimated by applying Kim et al.'s method [7]. (C) Estimated interaction functions of the significant causal connections. (D) Estimates of the non-stationary components of firing patterns. Symbols are as in Figs. 4.

Accounting for trial-by-trial variability

We have so far assumed that the stimulus-evoked responses of neurons are stereotyped and do not change across trials. However, while maintaining the same overall *shape*, the magnitude of neuronal firing patterns can often exhibit considerable variability across trials. It has been shown that these trial-by-trial variations can produce spurious patterns of Granger causality and this problem becomes even more severe when these variations are correlated across neurons [12, 13]. Fig. 6 shows an example of such problems in a very simple system composed of two simulated units. In this example, on each trial p, the activity of unit i was generated by means of an inhomogeneous Poisson process with firing probability $A_{i,p} \cdot \lambda_i(t)$, where the factor $A_{i,p}$ sets the overall magnitude of the response $\lambda_i(t)$ in trial p. The processes λ_1 and λ_2 were independent and both underwent a bell-shaped temporal modulation of their firing rates centered at $t = 1$ (Fig. 6 B). We set $A_{1,p} = A_{2,p}, \forall p$ to correlate the trial-by-trial variability of the two units (Fig. 6 C). Application of G-ETM recovered in this case an incorrect pattern of causal connectivity. This happened because, trial-by-trial changes in response magnitude produced additional variance in the data that could not be accounted for by the exogenous components of our G-ETM model (see the mismatch between the blue and black curves in Fig. 6 E). Therefore, the GLM fitting process attempted to explain this additional variance by means of the other available free parameters. That is, those related to interactions between neurons. Indeed, for this specific realization of spike trains, inclusion of fictitious causal influences $1 \rightarrow 2$, $2 \rightarrow 1$ and $2 \rightarrow 2$ significantly improved the percentage of explained variance (Fig. 6 F) thus producing an incorrect pattern of Granger connectivity.

To take into account correlated trial-by-trial variability in the magnitude of neuronal responses we extended our G-ETM model. To this end, we further augmented it with a set of $A_{i,p}$ additional parameters that model the response magnitude of neuron i in trial p (see Methods section for further details). Application of this new model (G-ETMV: Granger causality with Exogenous Temporal Modulations and trial-by-trial Variability) to the spike patterns in Fig. 6 B did not only recover the correct pattern of connectivity (compare Fig. 6 A and Fig. 6 G) but it also provided a faithful estimate of the response magnitudes $A_{i,p}$ across trial and neurons (Fig. 6 C). Furthermore, it also provided a more precise estimate of the exogenous temporal modulations of neuronal responses (Fig. 6 H). Taken together, results in Fig. 6 further support the notion that, in Granger causality, the presence of unaccounted variance (in this case trial-by-trial variability) can produce spurious patterns of functional connectivity.

We next validated our G-ETMV method by means of a series of Montecarlo simulations. These simulations had the same structure as those in Fig. 4 with the notable difference that, to produce correlated trial-by-trial variability the firing rates of all neurons were multiplied, on each trial, by the same factor randomly selected in the interval $[.5,\ 1.5)$. Consistent with the intuition provided by Figs. 6 application of our G-ETM method produced a false positive in 14 % of the cases; a value that is significantly above the set statistical threshold of $p < 0.05$ (Fig. 6). On the contrary, G-ETMV not only provided a significantly better estimate of the connectivity patterns (97 % vs. 92 % correct for the G-ETM and G-ETMV models respectively) but also maintained the percentage of false positives compatible with the set statistical threshold (6 %, Fig. 6). These results show that G-ETMV is an effective technique to estimate causal influences between neurons that exhibit exogenous temporal modulations in their firing rates whose magnitude is variable across trials and correlated across units.

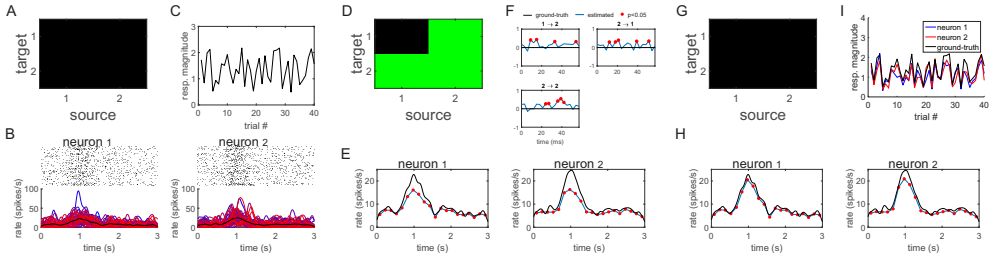

Figure 6. Trial-by-trial variability and Granger causality. The panel exemplify how trial-by-trial variability can affect Granger causality measures even when non-stationarity in firing rates is taken into account and how G-ETMV can successfully address this issue. (A) Ground-truth connectivity of our simple 2-neuron system (i.e. no connectivity). (B) Spike trains of the two independent units undergoing non-stationary changes in their firing rates and correlated trial-by-trial variability of response magnitudes. The red curves in the bottom panel represent the firing rate of the single trials, while the thick black line represents the average firing rate. (C) Ground-truth trial-by-trial variability of the responses of the two neurons. The black curve represents, for each trial, the overall level of activation of the two units. (D) In the presence of correlated trial-by-trial variability our G-ETM method recovers an incorrect connectivity pattern. (E-F) Ground-truth values (black curves) and estimates (blue curves) of the exogenous components of the firing rates (panel E) and of the interaction functions for the significant causal connections (panel F) recovered by G-ETM. (G-H) The correct patterns of connectivity (panel G) and exogenous components (panel H) are instead recovered by our G-ETMV method. (H) G-ETMV also provides a faithful estimate of the trial-by-trial response variability of both neurons.

Discussion

A fundamental goal of Neuroscience is to characterize the brain functional circuits underlying perception, cognition and action. Granger causality addresses this problem by detecting the flow of information between simultaneously recorded physiological signals [14]. In previous work, Kim and co-workers proposed a point-process extension of Granger causality that allowed to investigate functional connectivity directly at the spike train level [7]. As any *standard* Granger causality techniques also Kim et al.'s technique assumes that input time series are jointly stationary. That is, their temporal modulations must be entirely due to the series' past histories. This assumption is however rarely met in real neurophysiological experiments. Indeed, neuronal networks are characterized by a high degree of convergence and the activity of a given neuron is the result of the integration of the outputs of many, potentially thousands, projecting units, which is often not technically possible to concurrently record. Furthermore, brain networks often exhibit slow changes in their global state, which makes the magnitude of neuronal responses vary across trials and be correlated between units.

Here, we first showed that applying standard point-process Granger causality to spike trains that exhibit exogenous temporal modulations produces a non-negligible number of artefactual causal links between neuronal activities. In an experimental setting, these results would suggest the existence of fictitious connectivity patterns and would induce incorrect conclusions concerning the underlying information flow. To overcome these problems, we proposed here two novel point-process Granger causality techniques: G-ETM and G-ETMV. G-ETM is computationally less demanding and specifically designed for the case of spike trains exhibiting temporal modulations while G-ETMV is more computationally demanding but also handles the case of trial-by-trial, potentially correlated variability in neuronal responses. The choice of which one to use

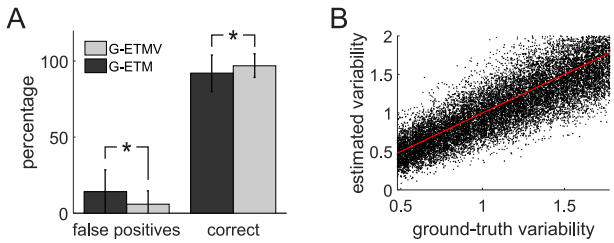

Figure 7. Montecarlo validation of G-ETMV. (A) Percentage of correct and false positive connections estimated by G-ETM and G-ETMV respectively when applied to spike trains exhibiting both exogenous temporal modulations and trial-by-trial variability. Montecarlo simulations have the same structure as in Fig. 6 A. (B) Scatterplot of estimated vs. ground-truth trial-by-trial variability coefficients (i.e. the terms $A_{i,p}$ in Eq. 6). The dots cluster around the unitary slope line (red line), indicating that estimates were close to their ground-truth values.

depends on a trade-off between available computational resources and a-priori hypotheses that the Experimenter has concerning a specific data set.

The jointly stationarity assumption gives Granger causality several appealing characteristics [14]. However, at the same time, it greatly limits its potential applications, as very often we are interested in investigating the information flow in brain networks undergoing stimulus-evoked state transitions whose causes are exogenous to the networks themselves. To extend Granger causality to these cases two main, not mutually exclusive, methods have been proposed in the literature. The first method consists in performing some form of pre-processing on the data to render them stationary and then apply Granger causality to this *new* stationary data set. For example, simple linear trends can be removed by differentiation while more complex non-stationary components can be removed by subtracting the ensemble average or the estimated evoked response from each trial [15, 16]. These techniques are however designed for time-continuous or continuously sampled data and cannot be directly applied to spike trains given their point-process nature. Furthermore, the removal of the ensemble average assumes that each trial is a realization of the same underlying stochastic process, an assumption that is not always met in practice [12]. The second method consists in using time-varying models to fit the data [17, 18]. These extensions to Granger analysis can effectively deal with time series exhibiting exogenous temporal modulations. However, they possess no underlying test statistics and thus significance of the estimated parameters and model comparison must be assessed by means of empirical and computation-intensive bootstrapping techniques [17, 18].

The Granger causality techniques proposed here overcome both problems. Since they directly model the neurons' CIF they can be applied to point-process data. Furthermore, they use time- and trial-dependent models of neuronal responses and can thus recover the correct patterns of directed connectivity from spike trains containing exogenous temporal modulations and trial-by-trial variability. Notably, both techniques use generalized linear models to estimate the underlying neuronal CIF. Thus, we could use the rich theoretical framework developed for this class of models and, particularly, the test statistics developed to assess the goodness-of-fit of a given model and the significance of the estimated parameters. This aspect was particularly relevant for Granger causality analysis as this technique is heavily based on model comparison. Finally, both G-ETM and G-ETMV produce an estimate of the effects of both observed and unobserved causes on neuronal responses. Thus, in addition to estimating functional connectivity, they can be also used to decompose the spiking activity of each unit into endogenous (i.e. observed) and exogenous (i.e. unobserved) components.

At the practical level, the results of our Montecarlo simulations stress the importance of carefully checking that the data set under scrutiny meets the assumptions of Granger causality [19]. Indeed, as shown in Figs. 1,3,4 B,6 D and 7 A, applying Granger causality analysis to spike trains that violate the assumptions of a given model produces a number of false positive (i.e. artefactual) connections well above the selected significance level. In these cases, incorrect conclusions might be drawn concerning the underlying connectivity pattern.

In summary, we presented here two novel point-process Granger analysis techniques, namely G-ETM and G-ETMV, that can correctly detect directed influences between neurons whose responses exhibit exogenous temporal modulations and correlated trial-by-trial variability. These novel techniques allow to investigate the information flow during stimulus-evoked periods and thus to reveal how neurons interact not only during baseline conditions, but also when their responses are modulated by exogenous stimulation.

Materials and methods

We first briefly review the point process Granger causality method proposed by Kim and co-workers [7].

A point process is a time series of discrete events that occur in continuous time [20]. Given an observation interval $(0, T]$, let $0 < u_1^i < \cdots < u_j^i < \cdots < u_{J^i}^i \leq T$ be a set of J^i spike times point process observations for $i = 1, \cdots, Q$ recorded neurons. Let $N_i(t)$ denote the number of spikes of neuron i in the time interval $(0, t]$ with $t \in (0, T]$. A point process model of a spike train is completely characterized by its conditional intensity function (CIF) λ_i, given the past spiking history $H_i(t)$ of all neurons in the ensemble:

$$\lambda_i(t|H_i(t)) = \lim_{\Delta \to 0} \frac{Pr[N_i(t+\Delta) - N_i(t) = 1|H_i(t)]}{\Delta} \tag{1}$$

where $H_i(t)$ denotes the spiking history of all the neurons in the ensemble up to time t including neuron i itself.

The function λ_i needs to be estimated from data. To this end, we first computed the history $H_i(t)$ of each neuron i in M_i non overlapping rectangular windows of duration W. We then denoted with $R_{q,m}$ the spike count of neuron q $(1 < q < Q)$ in the interval m $(1 < m < M_i)$ and used a generalized linear model (GLM) framework to model the logarithm of the CIF as a linear combination of the $R_{q,m}$ [21, 22]:

$$log\lambda_i(t|\gamma_i, H_i(t)) = \gamma_{i,0} + \sum_{q=1}^{Q} \sum_{m=1}^{M_i} \gamma_{i,q,m} R_{q,m}(t) \tag{2}$$

where $\gamma_{i,0}$ relate to a baseline level of activity of neuron i and the to-be-estimated interaction function $\gamma_{i,q,m}$ represents the effect of ensemble spiking history $R_{q,m}(t)$ on the firing probability of neuron i.

Casting the estimate of λ_i into an auto-regressive GLM framework allows an extension of Granger causality to point processes [7]. Indeed, following the definition of Granger causality, one can infer the potential causal connection $j \to i$ of neuron j onto neuron i by comparing the deviance of the full model in Eq 2 with that of a reduced model λ_i^j that excludes the effects of neuron j onto neuron i:

$$log\lambda_i^j(t|\gamma_i, H_i(t)) = \gamma_{i,0} + \sum_{q=1, q\neq j}^{Q} \sum_{m=1}^{M_i} \gamma_{i,q,m} R_{q,m}(t) \tag{3}$$

If both models describe the data well then the difference of their deviances can be asymptotically described by a chi-square distribution and one can then use the theoretical machinery developed for this distribution to infer statistical significance [7].

Accounting for temporally modulated spike trains

An assumption of standard Granger causality is that the examined stochastic processes are jointly stationary. That is, their temporal evolution must be entirely due to their past histories. To easily convince ourselves why this is the case, let us look at Eq. 2. In this equation, the CIF is assumed to depend, through the terms $R_{q,m}(t)$ only on the past history $H_i(t)$ of the neuronal ensemble. If the statistics of the spike trains are jointly stationary so are also the terms $R_{q,m}(t)$. This ensures that the GLM fitting process will converge to meaningful values for the parameters γ and that the difference of the deviances of models 2 and 3 will asymptotically follow a chi-square distribution. However, in the presence of spike trains exhibiting exogenous temporal modulations, the terms $R_{q,m}(t)$ will also be, in general, non-stationary and thus the GLM fitting process may converge to non-meaningful values or not converge at all. Furthermore, the model in Eq. 2 will, in general, no longer provide a good description of the data. As a consequence, the deviances of models 2 and 3 might no longer asymptotically follow a chi-square distribution. In this case, the problem of statistically comparing them may even become ill-posed.

To overcome this limitation we first need to understand the characteristics of temporal modulations in spike trains. Neurophysiological experiments are usually organized into trials. Within each trial, an experimental event occurs (e.g. a sensory stimulus is presented, a movement is performed, etc.) that produces modulations in neuronal activities. For data analysis purposes, the continuously recorded neuronal spike trains are then off-line segmented into trials centered around the presented experimental event. A common assumption in analyzing neuronal responses is that the modulations produced by the exogenous event has the same time-course and amplitude across trials. Under this assumption we can thus deal with this non-stationarity by explicitly including it in our model.

To this end, for each neuron i we subdivide the duration T of each trial into N_i non-overlapping windows of duration T/N_i. Within each window we then model the CIF as the sum of the to-be-estimated effect of an exogenous event (the experimental event) and the influences of the other neurons. Our model becomes thus:

$$log\lambda_i(t|\gamma_i, H_i(t)) = \alpha_{i,\lceil \frac{t}{T} N_i \rceil} + \sum_{q=1}^{Q} \sum_{m=1}^{M_i} \gamma_{i,q,m} R_{q,m}(t) \quad (4)$$

where $0 < t < T$ and the $\alpha_{i,c}$ (with $1 < c < N$) are a set of N_i additional parameters (one for each of the intervals in which we have subdivided a trial for neuron i) that explicitly model changes in firing rates due to exogenous effects (i.e. effects not due to interactions with self or other neurons).

Model parameters are estimated by means of a GLM fitting process and the potential causal influence of neuron j onto neuron i is assessed, similar to the method proposed by Kim et al. [7], by comparing the deviance of the model in Eq. 4 with that of a reduced model λ_i^j that excludes the effects of neuron j onto neuron i:

$$log\lambda_i^j(t|\gamma_i, H_i(t)) = \alpha_{i,\lceil \frac{t}{T} N_i \rceil} + \sum_{q=1, q\neq j}^{Q} \sum_{m=1}^{M_i} \gamma_{i,q,m} R_{q,m}(t) \quad (5)$$

Notably, the GLM fitting process provides not only an estimate of the interaction functions $\gamma_{i,q}$ but also of the exogenous modulations $\alpha_{i,c}$ of neuronal responses.

To select the values of M_i and N_i we repeated the fitting process using models having different values of M_i and N_i and we then selected the model that minimized Akaike's information criterion (AIC) [7, 23].

Accounting for trial-by-trial variability

We have so far assumed that stimulus-evoked responses are stereotyped and that their trial-by-trial variability is entirely due to a noise process. However, neuronal responses can exhibit considerable task-related variations across trials that cannot be captured by a noise process. Notably, correlated variations of response magnitudes can modulate cross-correlation or spectral coherence measures resulting in spurious patterns of Granger causality [12, 15]. To avoid these artifacts we need to explicitly include in our model potential trial-by-trial variations in response magnitudes. To this end, we added to our model a set of parameters $A_{i,p}$ that represents the amplitude of the non-stationary response component of neuron i in trial p:

$$log\lambda_{i,p}(t|\gamma_i, H_i(t)) = A_{i,p} + \alpha_{i,\lceil \frac{t}{T} N_i \rceil} + \sum_{q=1}^{Q} \sum_{m=1}^{M_i} \gamma_{i,q,m} R_{q,m}(t) \quad (6)$$

where $\lambda_{i,p}$ is the CIF of neuron i in trial p. Notably, the fitting process produces also an estimate of the parameters $A_{i,p}$ whose values can be used to assess the consistency of response magnitudes across trials. Also in this case, the potential causal influence of neuron j onto neuron i is assessed by comparing the deviance, across all trials, of the model in Eq. 6 with that of a reduced model $\lambda^j_{i,p}$ that excludes the effects of neuron j onto neuron i.

Generation of synthetic spike trains

For our simulations we set the temporal granularity to 1 ms. For each neuron i and trial p, spike trains were then generated by extracting, for each trial and 1 ms interval, a random number r uniformly distributed between 0 and 1. A spike was assumed to have occurred if $r \leq \lambda_{i,p}(t|\gamma_i, H_i(t))\Delta$ (where λ_i represents the time-dependent firing rate in spikes per second and $\Delta = 0.001\ s = 1\ ms$); otherwise, no spike was generated.

At each time t, the firing rate $\lambda_{i,p}$ was computed as:

$$\lambda_{i,p}(t) = A_{i,p} \cdot (\lambda^0_{i,p} + B_i e^{\frac{(t-\tau_i)^2}{\tau_0}}) \cdot \sum_{q=1}^{Q} \sum_{m=1}^{M_i} \delta_{i,q,m} R_{q,m}(t) \quad (7)$$

where $A_{i,p}$ models trial-to-trial variations of the activity of neuron i, $\lambda^0_{i,p}$ is a baseline level of activity, $B_i e^{\frac{(t-\tau_i)^2}{\tau_0}}$ is a non-stationary Gaussian-shaped modulation of the spike rate centered, within each trial, at time τ_i and with τ_0 determining its duration. The term $\sum\sum...$ represents the influence of all other neurons including neuron i itself. The network topology as well as the functional interactions between neurons are determined by appropriately setting the parameters $\delta_{i,q,m}$. In all our simulations we set $\tau_0 = 200\ ms$.

Author contributions

Conceptualization: AC, RTF and ENB; Funding Acquisition: AC and ENB; Investigation: AC; Methodology: AC; Writing - Original Draft Preparation: AC; Writing - Review and Editing: AC, RTF and ENB.

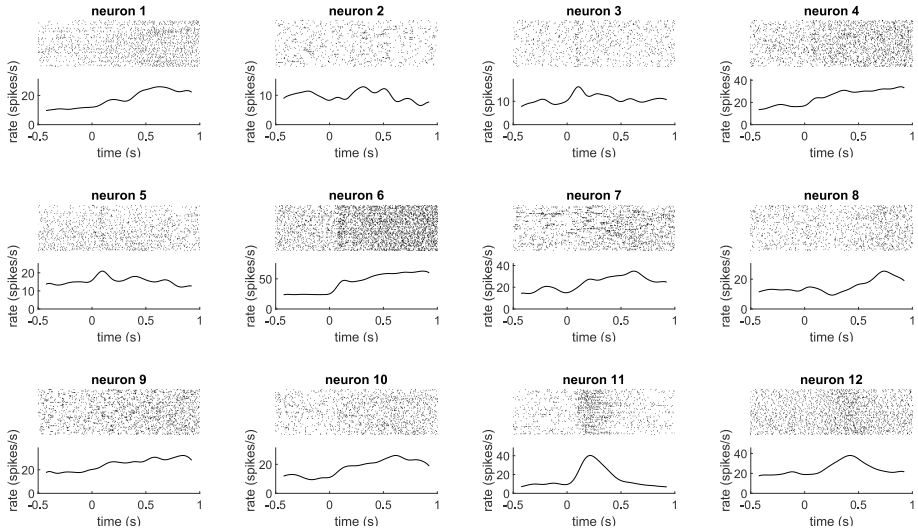

Figure S1. Spike trains recorded from the monkey pre-motor cortex (area F5) and included in our analysis. For each neuron, the upper panel shows the spike trains. Here, each row represents a trial and vertical lines mark the occurrences of spikes. The curve in the bottom panel represents the average, across all trials, of the neuron's firing rate.

Acknowledgments

We would like to thank John Assad for many stimulating discussions and Daniel Chicharro for providing enlightening comments on a preliminary version of this manuscript. This work was supported by a grant from the Harvard/MIT Joint Research Program to AC and ENB.

References

1. Jun JJ, Steinmetz NA, Siegle JH, Denman DJ, Bauza M, Barbarits B, et al. Fully integrated silicon probes for high-density recording of neural activity. Nature. 2017;551(7679):232–236. doi:10.1038/nature24636.

2. Zhou A, Santacruz SR, Johnson BC, Alexandrov G, Moin A, Burghardt FL, et al. A wireless and artefact-free 128-channel neuromodulation device for closed-loop stimulation and recording in non-human primates. Nature Biomedical Engineering. 2018;in press. doi:10.1038/s41551-018-0323-x.

3. Angotzi GN, Boi F, Lecomte A, Miele E, Malerba M, Zucca S, et al. SiNAPS: An implantable active pixel sensor CMOS-probe for simultaneous large-scale neural recordings. Biosensors and Bioelectronics. 2019;126:355–364. doi:10.1016/j.bios.2018.10.032.

4. Brody CD. Correlations without synchrony. Neural Computation. 1999;11(7):1537–51.

5. Gerstein GL, Perkel DH. Simultaneously recorded trains of action potentials: analysis and functional interpretation. Science. 1969;164(3881):828–30. doi:10.1126/science.164.3881.828.

6. Gerstein GL, Perkel DH, Dayhoff JE. Cooperative firing activity in simultaneously recorded populations of neurons: Detection and measurement. Journal of Neuroscience. 1985;5(4):881–889.

7. Kim S, Putrino D, Ghosh S, Brown EN. A Granger causality measure for point process models of ensemble neural spiking activity. PLoS Computational Biology. 2011;7(3):e1001110. doi:10.1371/journal.pcbi.1001110.

8. Granger CWJ. Investigating causal relations by econometric models and cross-spectral methods. Econometrica. 1969;37(3):424–438.

9. Chicharro D, Ledberg A. When two become one: The limits of causality analysis of brain dynamics. PLoS ONE. 2012;7(3). doi:10.1371/journal.pone.0032466.

10. Casile A. Mirror neurons (and beyond) in the macaque brain: An overview of 20 years of research. Neuroscience Letters. 2013;540:3–14. doi:10.1016/j.neulet.2012.11.003.

11. Churchland MM, Yu BM, Ryu SI, Santhanam G, Shenoy KV. Neural variability in premotor cortex provides a signature of motor preparation. Journal of Neuroscience. 2006;26(14):3697–3712. doi:10.1523/JNEUROSCI.3762-05.2006.

12. Truccolo WA, Ding M, Knuth KH, Nakamura R, Bressler SL. Trial-to-trial variability of cortical evoked responses: implications for the analysis of functional connectivity. Clinical Neurophysiology. 2002;113(2):206–26. doi:10.1016/S1388-2457(01)00739-8.

13. Wang XJ. Decision making in recurrent neuronal circuits. Neuron. 2008;60(2):215–234. doi:10.1016/j.neuron.2008.09.034.

14. Seth AK, Barrett AB, Barnett L. Granger causality analysis in neuroscience and neuroimaging. Journal of Neuroscience. 2015;35(8):3293–3297. doi:10.1523/JNEUROSCI.4399-14.2015.

15. Wang X, Chen Y, Ding M. Estimating Granger causality after stimulus onset: A cautionary note. NeuroImage. 2008;41(3):767–776. doi:10.1016/j.neuroimage.2008.03.025.

16. Chen Y, Bressler SL, Knuth KH, Truccolo WA, Ding M. Stochastic modeling of neurobiological time series: Power, coherence, Granger causality, and separation of evoked responses from ongoing activity. Chaos. 2006;16(2):1–8. doi:10.1063/1.2208455.

17. Hesse W, Möller E, Arnold M, Schack B. The use of time-variant EEG Granger causality for inspecting directed interdependencies of neural assemblies. Journal of Neuroscience Methods. 2003;124(1):27–44. doi:10.1016/S0165-0270(02)00366-7.

18. Ding M, Bressler SL, Yang W, Liang H. Short-window spectral analysis of cortical event-related potentials by adaptive multivariate autoregressive modeling: data preprocessing, model validation, and variability assessment. Biological Cybernetics. 2000;83(1):35–45. doi:10.1007/s004229900137.

19. Dang S, Chaudhury S, Lall B, Roy PK. Assessing assumptions of multivariate linear regression framework implemented for directionality analysis of fMRI. Proceedings of the Annual International Conference of the IEEE Engineering in Medicine and Biology Society, EMBS. 2015;2015-Novem:2868–2871. doi:10.1109/EMBC.2015.7318990.

20. Daley DJ, Vere-Jones D. An introduction to the theory of point processes. New York, NY: Springer; 2003. Available from: http://www.springerlink.com/content/978-0-387-21337-8.

21. Truccolo W, Eden UT, Fellows MR, Donoghue JP, Brown EN. A point process framework for relating neural spiking activity to spiking history, neural ensemble, and extrinsic covariate effects. Journal of Neurophysiology. 2005; p. 1074–1089. doi:10.1152/jn.00697.2004.

22. Okatan M, Wilson MA, Brown EN. Analyzing functional connectivity using a network likelihood model of ensemble neural spiking activity. Neural Computation. 2005;17:1927–1961. doi:10.1162/0899766054322973.

23. Akaike H. A new look at the statistical model identification. IEEE Transactions on Automatic Control. 1971;19(716-723).